# SPECTROPHOTOMETRY FROM FIBER SPECTRA AND BROADBAND COLORS: APPLICATION TO THE SDSS

James E. Gunn *et. al.*

**Abstract:**

Fiber spectrographs typically have sensitivity in wavelength which is strongly modulated by atmospheric differential refraction. In this paper we investigate the detailed form of this modulation and investigate the extent to which broadband photometry covering the wavelength range of the spectra can be used to recover spectrophotometric information. For the parameters and errors relevant to the Sloan Digital Sky Survey spectrographs and photometric system, RMS spectrophotometric errors of about 3 percent over most of the relevant seeing and airmass ranges are achievable with very simple algorithms. The errors are strongly limited by the broadband photometric errors for the survey and can be improved if the accuracy of that calibrating photometry is improved.

## I. Introduction

It is well known that slit spectroscopy and fiber spectroscopy in general do not yield spectrophotometrically accurate results, because differential refraction causes a spread of a few arcseconds on the sky in the elevation of a source over the typical free spectral range of a spectrograph. These differently located monochromatic images do not illuminate the slit or fiber in the same way, and light at the wavelength extremes is typically more attenuated than the light at the central wavelength. If the image is guided at a wavelength such that the refractive spread is symmetric about that wavelength, the fiber cuts off the seeing wings (or even the body of the PSF for small fibers) symmetrically, but typically fiber placement errors and guiding errors prevent even this case from holding in any detail. For a multifiber spectrograph covering a large field, there will be in addition be differential guiding errors over the field and errors caused by traversing elevations during the exposure different from the one for which the fiber placement was designed.

In the Sloan Digital Sky Survey (hereinafter SDSS) more than a million high-quality CCD spectra will be obtained of galaxies, stars, and quasars, along with CCD surface photometry in five bands. It would clearly be of enormous interest to obtain spectrophotometry of these objects using these spectra. We have attempted in the past to calibrate them using "smears", short-exposure spectra taken with the telescope moving to synthesize an aperture about twice the linear size of the three-arcsecond fibers. This effort has been less than successful both because of inherent geometric problems with the procedure for extended sources with structure (Tremonti et al 2004) and the inadequate signal-to-noise of the smear exposures. In the SDSS, however, we also have accurate CCD surface photometry, and 3 of the bands ($g$, $r$, and $i$) both lie almost completely within the 3900-9000 Å free spectral range of the spectrographs and pretty much cover that range. It does not seem out of the question to use the broad-band photometry to help recover the spectrophotometry, and this paper addresses ways to accomplish this.

There are clearly several parts to the problem and we will address them in turn. The first is to investigate for realistic PSFs, centering errors, and airmass ranges the *form* of the fraction of the energy lost at the fiber edge as a function of wavelength. This loss, expressed in magnitudes, we will call the *loss function* $L(\lambda)$. We will adopt a new independent variable which is linear in the differential refraction, and show that in this variable the loss function is, over a wide range in conditions, quite accurately representable as a least squares fit to a simple quadratic. This gives us some hope, because the three coefficients which describe a quadratic polynomial should be determinable with the three broadband magnitudes, or, rather, the differences between the measured magnitudes and those synthesized from the uncorrected fiber spectra. This approach then uses ONLY these differences as inputs, and requires no detailed knowledge of the centering, seeing, or intrinsic image profile for the object in the fiber in question.

One must then work out how to determine the coefficients from the magnitude differences, and, once determined, answer the question of how accurately *this* quadratic represents the desired function. It will certainly *not* be precisely the least-squares fitting polynomial, since it is determined by only three (peculiarly spaced, as we shall see) averaged values.

Finally, the accuracy of the whole process is degraded because the photometry itself is not perfect, and the way the photometric errors propagate into the solution must be investigated. It is also certainly true that spectrophotometry cannot be done without standard stars, and the way that the standardization procedure in general and specifically as performed in the SDSS must be considered in this process.

## II. The Loss Function

Atmospheric differential refraction is described in several places (eg Allen, 1963), whose polynomial form we will use here. It is reasonably accurately ( 1%) represented by the simple form

$$D(\lambda) = -\rho \left( \frac{\lambda_0^2}{\lambda^2} - 1 \right) \tan z. \tag{1}$$

where $D$ is the zenith angle difference between an image at wavelength $\lambda$ and one at the reference wavelength $\lambda_0$, and $z$ is the zenith angle. For an observatory at the altitude and with the average temperature of Apache Point, the amplitude $\rho$ is approximately 0.94 arcseconds for a reference wavelength of $\lambda_0 = 5060$ Å, which is the 'central' wavelength (in the sense that it splits the difference in the refraction at the ends) for the 3900-9000 Årange in this approximation. The *real* central wavelength using accurate refraction is $\lambda_0 = 5018$ Å. In the calculations that follow we have used the more accurate polynomial form and central wavelength, but the choice makes no significant difference to anything we will discuss.

Since the differential refraction is a very nonlinear function of wavelength, we introduce at the outset a variable which is linear in the refraction:

$$X(\lambda) = \frac{D(3900) + D(9000) - 2D(\lambda)}{D(3900) - D(9000)} \tag{2}$$

This function has values -1 at 3900Å, 1 at 9000Å, and is clearly linear with refraction between. It has value zero at the central wavelength. If $D_{max}$ is defined as $[D(3900) - D(9000)]/2$ (0.64 arcsec for APO at 45° elevation), then

$$D(\lambda) = D_{max} X(\lambda).$$

In order to study the loss function, one must clearly know what the shape of the PSF and the object is and their sizes relative to that of the fiber. We adopt the standard double-gaussian approximation to the Kolmogorov PSF, (Racine, 1996) so a star image has radial brightness distribution

$$PSF(r) = C[\alpha e^{-r^2/2\sigma_0^2} + (1-\alpha)e^{-r^2/2\sigma_1^2}], \tag{3}$$

where $\alpha \simeq 0.9$ and $\sigma_1/\sigma_0 \simeq 2$. The FWHM of this function is very nearly equal to $2.5\sigma_0$, and we will use this FWHM (hereinafter simply the 'seeing') to scale the seeing models.

We built a sequence of models with seeing-convolved exponential profiles (to represent disk galaxy models) and deVaucoleurs profiles (to represent early-type galaxies) in a range of sizes and flattenings with a PSF as approximated above with $\sigma_0 = 3$ pixels, $\sigma_1 = 6$ pixels, and $\alpha = 0.9$, for exploration of the effects, and a three times higher resolution set for accurate calculations. The effects of different seeing were handled by changing the assigned pixel scale in arsec/pixel and hence size of the 3 arcsecond fiber aperture placed on these images; the image scale itself was not changed. It soon became apparent, as one would naively expect, that galaxies are in general much less adversely affected than are the stars, and we will concentrate on the effects on stars. It is only the case in which the seeing is very good and the centering errors and zenith angle are small so that there is very little spillover that the galaxies have worse errors than the stars, and even in these cases they are well correctable. We will return to some of these questions later when we present the results in more detail.

Given these models and an assumed seeing, one can place a three-arcsecond fiber aperture on an assumed center and measure the amount of flux entering the fiber. One can do this at the central wavelength and on a net of wavelengths covering the free spectral range of the spectrographs, offsetting the center of the aperture vertically (in elevation, y in our focal plane coordinate system) by $D(\lambda)$. If we let F(x,y) be the flux within the fiber aperture for an image of unit total flux when the center of the image is at x,y (in arcseconds, say) relative to the center of the fiber, then we define the loss function L($\lambda$) for a given image which is at x,y in the fiber at $\lambda_0$ as

$$L(\lambda) = -2.5log_{10}F(x, y + D(\lambda))/F(0,0). \tag{4}$$

If we knew the flux calibration for light entering the fiber perfectly, then clearly subtracting the loss function from the observed SED expressed in AB magnitudes would yield the correct SED for the object observed with a centered aperture of the diameter of the fiber with no refractive losses.

At this point it is probably well to review our assumptions, stated and hidden. There is typically a small gradient in seeing, proportional to $\lambda^{-0.2}$, from Kolmogorov effects, which we could have included but ignore for simplicity. Far more serious is the assumption that the image has no spectrophotometric gradients; that is, the image has an unrefracted brightness distribution on the sky which is representable by

$$B(x, y, \lambda) = b(x, y)S(\lambda),$$

at least on scales comparable to the differential refraction. This is certainly true for point sources (except for the Kolmogorov effects alluded to above), is probably true to the required accuracy for most galaxies, but is certainly NOT true for such objects as faint AGNs in relatively bright galactic nuclei. For these objects more sophisticated techniques in which one uses the measured surface brightness and color profiles must be used to achieve reasonable accuracy. We will discuss some possible schemes later, but will not develop them in any detail.

A reasonable way to visualize the loss function is to plot $F(x,y)/F(0,0)$ over the full diameter of the fiber in $y$ for a few values of $x$. For a given airmass and centering, the loss function, expressed as a function of $X$, is simply a segment of one of these curves from $y - D_{max}/2$ to $y + D_{max}/2$, $X = -1$ to $X = 1$. Figure 1 shows such a set of curves and the lengths of the segments for a set of airmasses and values of the seeing FWHM.

It is clear that the curves are smooth and in most cases likely well representable by a piece of a parabola, *as a function of* $X$ except in the cases of good seeing and high airmass, where it is somewhat less obvious. Because there are so many variables involved, it is not quite clear how to ask the question of how well we can do with a parabolic approximation, or any other for that matter. We will characterize the errors in this and later, more directly relevant quantities by a set of simple simulations. For a given seeing value, central wavelength image locations are chosen to cover a net centered on the fiber, one point per pixel in the simulation, of size large enough that points out to three standard deviations $\sigma_l$ of an assumed gaussian error distribution for the image center locations are included. The loss functions for a given airmass are calculated for each of these locations, and the rms error for a least-squares parabolic fit obtained. These are weighted by the gaussian centering error distribution, and a somewhat peculiar quantity, the mean rms error, is obtained. This is repeated for a sequence of airmasses and seeing values. Typical curves for this quantity for a one-dimensional fiber location standard deviation of 300 milliarcseconds (mas), which is a typical value experienced in the SDSS, are plotted in Figure 2 for a star for airmasses between 1 and 2 and seeing between 1 and 2 arcseconds. The errors inherent in this approximation are clearly very small.

However, the fact that the loss function is accurately representable by a least-squares parabolic function of X, while encouraging, is not enough. We certainly do not have the whole loss function to fit, and if we did, we would not need the parabolic approximation. Instead we have measured magnitudes for which we know the response functions and can calculate them from our spectrum. The differences between the measured and synthesized magnitudes are essentially three averaged points, appropriately weighted, on the loss function. These three values certainly define a parabola, but it will not be exactly the same parabola as the excellently-fitting least-squares one. This is the next thing we need to look into.

## III. Approximating the Loss Function from Color Errors

The photometric response functions for the SDSS for the $g$, $r$, and $i$ bands plotted as functions of $X$, not $\lambda$, are shown in Figure 3. We see immediately that whereas the $r$ and $i$ bands define nicely limited ranges in $X$, the $g$ band covers an enormous range, and it is clear that the 'equivalent X' value for $g$ will depend very much on the spectrum of the object in question. Thus we need to be very careful when we solve for the loss function.

For each band $x = (g,r,i)$, we can define for an object with SED $f_\nu(\lambda)$ the synthetic filter flux $f_x$

$$f_x = \int f_\nu S_{x\nu} \frac{d\lambda}{\lambda}, \tag{5}$$

where $S_{x\nu}$ is the normalized response function for the filter $\int S_{x\nu} d\lambda/\lambda = 1$. The response function is proportional to the DQE of the system; *i.e.* the probability that a photon of frequency $\nu$ is converted to a detected photoelectron in the CCD, and contains the atmospheric transmission, the telescope transmission, the filter transmission, and the detector quantum efficiency. The $S_{x\nu}$s are accurately known for the SDSS system, and if we let $l(X) = 10^{-.4L(X)}$ be the multiplicative *loss factor*, then we can calculate from the observed spectrum, which is $f_\nu l(X)$ the spectrophotometric filter flux

$$f_{Sx} = \int f_\nu l(X) S_{x\nu} \frac{d\lambda}{\lambda} \tag{6}$$

If we define the *effective* $X$ for filter $x$ as

$$\bar{X}_x = \frac{\int f_\nu S_{x\nu} X \frac{d\lambda}{\lambda}}{f_x}$$

and the effective $X$ variance for filter $x$ as

$$\langle (X - \bar{X}_x)^2 \rangle_x = \frac{\int f_\nu S_{xx\nu} (X - \bar{X}_x)^2 \frac{d\lambda}{\lambda}}{f_x}$$

then we can expand the expression for $f_{Sx}$ as follows:

$$f_{Sx} = \int f_\nu (\bar{l} + (X - \bar{X}_x) \frac{dl}{d\bar{X}_x} + \frac{1}{2}(X - \bar{X}_x)^2 \frac{d^2 l}{d(\bar{X}_x)^2} + \ldots) S_{x\nu} \frac{d\lambda}{\lambda},$$

where $\bar{l} = l(\bar{X}_x)$, and $dl/d\bar{X}_x$, etc, is shorthand for $dl/dX(X = \bar{X})$.

Note that this expression has nothing to do with our assumption that the loss function $L(X)$ is quadratic; it only requires that over the main width of filter $x$ the loss ratio $l(X)$ is reasonably accurately quadratic.

The first-order term vanishes, and we are left, after converting to magnitudes, with

$$m_{Sx} \simeq m_x - 2.5 log_{10} \bar{l} - 2.5 log_{10} (1 + \frac{1}{2} \langle (X - \bar{X}_x)^2 \rangle_x \frac{d^2 l}{d(\bar{X}_x)^2}).$$

$$\simeq m_x - 2.5 log_{10} \bar{l} - \frac{1}{2\gamma \bar{l}} \langle (X - \bar{X}_x)^2 \rangle_x \frac{d^2 l}{d(\bar{X}_x)^2},$$

where $m_{Sx}$ is the magnitude corresponding to the synthesized filter flux $f_{Sx}$. The first-order expansion of the logarithm here is an excellent approximation.

We now assume that the loss function $L = 2.5 \log_{10} l$ is quadratic:

$$l = 10^{-.4(a+bX+cX^2)} = e^{-\gamma(a+bX+cX^2)},$$

$\gamma = 0.4 \ln 10 = 0.921$.

After a bit of manipulation to evaluate the derivatives, we find

$$m_{Sx} - m_x = a + b\bar{X}_x + c[(\bar{X}_x)^2 + \langle (X - \bar{X}_x)^2 \rangle_x] - \frac{\gamma \langle (X - \bar{X}_x)^2 \rangle_x}{2} (b + 2c\bar{X}_x)^2. \tag{7}$$

The last term is typically less than .001 magnitude and will be neglected. Clearly the term multiplying the $c$ coefficient is just $\langle X^2 \rangle_x = \bar{X^2}_x$, defined in the obvious way, so we find, finally, the simple expression

$$m_{Sx} - m_x = a + b\bar{X}_x + c\langle X^2 \rangle_x \tag{8}$$

for $x = g, r, i$. This is a set of equations which can be solved for the coefficients if we know the relevant moments of $X(\lambda)$ over the filters and spectrum of the object.

We can take either of two approaches to the moments. For ordinary stars, the value of $\bar{X}_x$ and $\langle X^2 \rangle_x$ are very tightly correlated with the colors, the $g$ moments with $g - r$, the $r$ and $i$ moments with $r - i$. As expected, the $r$ and $i$ moments vary very little with color, since they are 'narrow filters' in $X$ space, but the variation of both the mean $X$ and the mean $X^2$ vary a great deal for $g$. The variation is illustrated in Figure 4 for the stars in the Gunn-Stryker (GS, 1984) spectrophotometric atlas. Quadratic fits to the relations are more than adequate, and we get

$$\begin{aligned}
\bar{X}_g &= -0.245 + 0.1060(g-r) - 0.0081(g-r)^2 \\
\langle X^2 \rangle_g &= 0.146 - 0.0739(g-r) + 0.0131(g-r)^2 \\
\bar{X}_r &= 0.488 + 0.0340(r-i) - 0.0072(r-i)^2 \\
\langle X^2 \rangle_r &= 0.250 + 0.0323(r-i) - 0.0064(r-i)^2 \\
\bar{X}_i &= 0.796 + 0.0152(r-i) + 0.0002(r-i)^2 \\
\langle X^2 \rangle_i &= 0.638 + .0243(r-i) + 0.0004(r-i)^2
\end{aligned} \tag{9}$$

excluding carbon stars and very cool giants with $r - i > 2.0$ from the fit. It is clear that these fits are very tight; what is less clear is how good they need to be. A test with random gaussian errors of .02 in $\bar{X}_g$ and $\langle X^2 \rangle_g$, which are pessimistic estimates of the scatter in the plots, added into the moments before solving for the coeffients yielded negligible increases in the error estimates. Thus these relations are good enough for ordinary stars and almost certainly also so for ordinary galaxies over the redshift range observed by the SDSS. They are hopelessly bad for stars with weird spectra, very red objects with complex spectra, and quasars and other emission line objects.

A more nearly self-consistent way to find the moments, however, which makes no use of any assumptions about the nature of the object, is simply to *calculate* the moments from the observed spectrum. One does not know the loss function at the beginning, but the moments are not terribly sensitive to it unless it is quite extreme, and if there is any doubt one can iterate. One has to calculate the spectrophotometric magnitudes anyhow, and adding the calculation of the moments is a trivial complication.

So we are now in a position to calculate $a$, $b$, and $c$ from Equation (7). As stressed before, this quadratic is NOT the same one as obtained from least-squares fitting over the whole range of $X$. How well does it allow us to do spectrophotometry?

## IV. Spectrophotometric errors using this algorithm

One could if one wished take real spectra, combine them with theoretical loss functions, calculate the moments, and simulate the whole process. We have chosen to do something simpler which is essentially equivalent. For the set of GS stars we calculate the mean values of the $\bar{X}$s and $\bar{X}^2$s and fit a linear relation for those as functions of $\bar{X}_g$ (as a surrogate for color). The mean value of $\bar{X}_g$ of -0.19 corresponds to objects of the color of late G stars, near the mean color of SDSS objects. Values near -0.3 correspond to blue objects like A stars or low-redshift quasars, and values near -0.1 to red objects like middle M dwarfs. The linear relations are (including a tautological one for $\bar{X}_g$)

$$
\begin{aligned}
\bar{X}_g &= -0.190 + 1.0(\bar{X}_g + 0.19) \\
\langle X^2 \rangle_g - (\bar{X}_g)^2 &= 0.074 - 0.24(\bar{X}_g + 0.19) \\
\bar{X}_r &= 0.495 + 0.157(\bar{X}_g + 0.19) \\
\langle X^2 \rangle_r - (\bar{X}_r)^2 &= 0.0116 - 0.328(\bar{X}_r - 0.495) \\
\bar{X}_i &= 0.800 + 0.071(\bar{X}_g + 0.19) \\
\langle X^2 \rangle_r - (\bar{X}_i)^2 &= 0.0043
\end{aligned}
\tag{10}
$$

These fits are not terribly good, but indicate the range over which the $\bar{X}$s and the widths of the loss function integrands vary with color, which for the present purposes is all we care about.

We simply use these as representative values. In detail, we take each loss function calculated in the simulations above (not the quadratic approximation), and evaluate the corresponding loss ratio. This is integrated with a gaussian in X centered on $\bar{X}$ for that color and of width $\sigma$ equal to the corresponding centered second moment in $\bar{X}$ from the relations above to mimic the averaging over the filter. We concentrated on stars of about the mean color, but investigated the effects of color. It is clear that color will have little effect in $r$ and $i$, but red stars have $\bar{X}_g$ closer to zero and have a smaller width of the kernel, both decreasing our ability to define the loss function in the blue; we thus confidently expect the errors in the blue to be worse for red objects than for blue ones.

The rms errors for stars of mean color at several different seeings and airmasses is presented in Figure 5. A comparison with Figure 2 shows that, indeed, the errors are considerably worse than those reflected in the least-squares fit polynomials, by factors of about 2-3. The errors for red stars, with $\bar{X}_g \sim -0.1$ are about 25% worse; those for blue stars with $\bar{X}_g \sim -0.3$, about 25 percent better, than for these stars of mean color.

There is, however, another source of error which we must consider, namely the fact that the measured magnitudes have errors themselves *and* that the magnitudes synthesized from the spectra have errors. Thus the magnitude differences, which determine the polynomial coefficients, have errors. The errors in the synthetic magnitudes arise primarily from photon noise and will be neglected here; they are, in fact, negligible. At the brightnesses relevant to the SDSS spectroscopic sample, the broadband photometry is currently dominated by systematic error associated with calibration uncertainties and is in the neighborhood of 2 percent for both colors and fluxes. We will in what follows ignore the overall flux uncertainty; it certainly enters what one would like to call "spectrophotometry", but we are primarily interested here in the *shape* of the spectrum, and one can in any case simply add the overal flux error in quadrature if one wishes. The effect of color errors is quite simple; they propagate linearly through the solution of the system in equation 7, and one finds that the rms photometric error $\sigma_P$ is, approximately,

$$\sigma_P^2 = \sigma_{P0}^2 + 1.1\sigma_{(g-r)}^2 + 0.8\sigma_{(r-i)}^2, \tag{11}$$

where $\sigma_{P0}$ is the spectrophotometric error with no broadband photometric errors. For color errors of .02, which is the current level of accuracy of the SDSS photometry, this puts a floor of about 2.8 percent on the spectrophotometric errors for stars of mean color. The errors including the color errors for the same conditions as those illustrated in Figure

5 are seen in Figure 6.

Conditions at the SDSS site at Apache Point sometimes include good seeing and transparency good enough for spectroscopy but not imaging (Imaging is conducted only under conditions of good seeing and good transparency, and preempts spectroscopy), but not often. Ninety percent of all spectroscopic work has been conducted with seeing greater than 1.4 arcseconds, 98 percent greater than 1.3, with a median near 1.9. Ninety percent of the data have been taken at airmasses of 1.4 or less, 98 percent at 1.5 or less. It is clear under these conditions from Figure 6 that the errors in spectrophotometry are almost always dominated by the broadband photometric errors and seldom exceed the roughly three percent floor imposed by them. One can reasonably ask whether one might be making a mistake using the broadband magnitudes at all—clearly if the fiber losses are small enough, one will be worsening the situation using the broadband magnitudes, with their attendant errors, to calibrate. That this is not the case is seen in Figure 7, where the rms deviation of the loss function from its mean value, which is just the spectrophotometric error if no correction is made, is plotted for the same conditions as for Figure 6. The average improvement is of order a factor of three using the broadband magnitudes to calibrate. In addition, the uncorrected errors are very strong functions of the observing airmass, which would introduce serious systematics in the data.

It is also painfully clear that under these typical conditions for spectroscopy, better broadband photometry will result in better spectrophotometry. Figure 8 shows the spectrophotometric errors for color errors of 0.01 magnitude, and if the photometry could be improved to this level (for which there is some hope) the spectrophotometric errors using the algorithms developed here would decrease to the $\sim$ 1.5 percent level.

**V. Standardization**

Before any of this is done, it is necessary to put the spectra on some sort of approximate energy scale; we cannot hope that the instrumental response will be simple enough that one can start with raw instrumental spectra. What we have done, after all, is to show that we can represent the refractive loss function simply and well, nothing more complex. In order to do this one must use standards of some sort. In the SDSS, halo F stars are used, the prototypical object being the fundamental spectrophotometric standard $+17°4708$, though the typical stars actually used are somewhat cooler and more metal-rich (Tremonti et al 2004). As described there, the spectra of these stars are corrected to models derived from their spectral features, and the mean correction which does this is applied to all the spectra. In the current context, it is clear that this process corrects for all instrumental effects *including the loss function* for these stars. Thus to the extent that the plate is accurately drilled, the guiding very good, the airmass near the design one, and all sources are point sources — *i.e.* that the loss function is the same for all sources on the plate—the standardization will correct for the refractive losses. This is, unfortunately, not the case, but the fact that the gross features of the loss function *are* already removed probably improves the situation.

How does this standardization procedure interact with using broadband colors? What should be done with the colors of the standards? The answers to these questions depend on how well the magnitude system is calibrated in terms of absolute spectrophotometry—that is to say, how well the system offsets to an AB system are known. If the relations between the broadband magnitudes and the flux integrals defined in Equation (6) are accurately known, then it is appropriate to force the spectrophotometry of the standards to their measured colors. This can be done using the quadratic techniques developed here, or, much better, using the colors as constraints when fitting the models to the spectra. The current situation with the SDSS colors (and almost all other systems) is such that the AB corrections are *not* very well known. In this case, the differences between the synthetic magnitudes and measured ones of the standards need to be applied to all the measured magnitudes. One of these MUST be done, or the differences between the measured colors and the synthetic ones for the standards will lead to the spectrophotometry not being on the system of the standards. If it is the case that the systematic photometric errors are uniform over a plate, this "local" determination of the offsets can, in principle, *determine* the photometric errors to some level of accuracy and thus reduce their impact on the spectrophotometry. At the present time, given the nature of the uncertainties, this "local" application of the offsets would appear to be the best way to proceed.

If the standards are reduced and classified in a uniform way and the photometric errors are unbiassed, eventually a set of AB corrections, essentially some weighted mean for all the observations, will emerge. The application of these corrections will provide a robust connection between the photometry and the spectrophotometry as defined by the models used for the standard stars. It appears likely at the moment that the errors in the F star models and uncertainty in the AB corrections for the SDSS system are comparable at the level of two to three percent.

## VI. Summary

We have shown that for instrumental parameters similar to those of the SDSS the losses inherent in fiber spectroscopy can be well represented by simple functions of the refraction parameter $X(\lambda)$. Those functions can be well determined by using the differences between synthetic broadband magnitudes derived from the spectra and measured broadband fiber aperture magnitudes (provided, of course, that you have the latter). The resulting RMS errors for observing parameters typical of the SDSS are are about half again as large as the broadband color errors; the corrections for fiber losses are sufficiently good that the spectrophotometric errors are dominated by the broadband errors for typical observing conditions.

It is to be noted that the procedure uses no *a priori* information about seeing, airmass, centering, or object image size. It uses *only* the synthetic magnitudes and the measured ones. It is clear that one could, in principle, do better with a detailed analysis of the broadband images, calculating for each image the footprint of the fiber for each wavelength and doing the appropriate average, and taking account of the seeing difference between the time the spectroscopy was done and the time the imaging was done. Since there is no *a priori* knowledge of the exact fiber centering, that would have to be fitted, using the tilt of the spectrum for centering along the dispersion and perhaps its curvature for centering perpendicular. In any case the procedure would be very involved and one could not expect the color-related errors to be much better than for the simple procedure described here.

For objects which are geometrically and spectrophotometrically complex, in the sense of having very strong spectral gradients over small angular scales, it is clear that any procedure utilizing only the fiber spectrum and broadband images cannot be expected to yield accurate spectrophotometry. The situation may or may not be hopeless; such techniques as principal component analyses might be used, for example, to separate a faint AGN spectrum from that of the stars in the nucleus of the host galaxy. If the fibers are placed very accurately relative to one another (as they are for the SDSS) the loss function determined from nearby point sources in the field gives a good approximation for that for the nucleus, and one can proceed using that information and a stellar component reflecting the color of the galaxy and the stellar features in the spectrum. It is not clear that any general, "pipelineable" procedure can be devised to handle such cases without a quite large expenditure of effort. For the vast majority of objects, however, we have shown that the simple procedure outlined here will produce excellent results.

## References

Allen, C. W., 1963, *Astrophysical Quantities*, second edition, Athlone, London, 119
Racine, R., 1996, PASP 108, 699
Tremonti, C., 2004, in preparation
Gunn, J. E., & Stryker, L, 1983, Ap. J. (Suppl.) 52, 121.

## Figure Captions

Figure 1.
Fractional loss for three values of the seeing FWHM for various locations of the center of the PSF on a 3-arsecond fiber. The uppermost of the three sets of curves are for a star centered in x; the y range is from one edge of the fiber to the other. The differentially refracted spectrum of a starlike object spans a part of this curve of length shown in the lower center for various airmasses. The lower two sets of curves are for a star off center horizontally by 0.5 and 0.75 fiber radii. The curves are approximately parabolic in all cases; only in the case of very good seeing, good centering, and large airmass are there obvious quartic deviations over the relevant range.

Figure 2.
Least squares fitting errors resulting from a parabolic fit to the loss function for various seeing values (the curve labels) and airmasses (the abscissa) for a population of starlike objects with a 2-D gaussian distribution of image centers on a 3-arcsecond fiber with a sigma of 300 milliarcseconds. The values plotted are the mean over the population of image centers of the RMS fitting errors. For airmasses of 1.5 or smaller, for which almost all of the SDSS spectroscopic data have been taken, the loss function is representable by a parabola to better than 0.7 percent RMS.

Figure 3.
The quantum efficiency curves for the three SDSS filters $g$, $r$, and $i$ plotted as functions of the refraction variable $X$. More than half the total refraction range is contained within the $g$ filter, so it is clear that the weight of $g$ in fitting the loss function will be quite sensitive to the distribution of flux in the $g$ filter.

Figure 4.
Six panels showing the moments $\langle X \rangle$ (called $\bar{X}$ in the text) and $\langle X^2 \rangle$ for the three SDSS colors $g$, $r$, and $i$, as functions of color. These points were calculated using the stars in the Gunn-Stryker spectrophotometric atlas. Plusses are dwarfs, diamonds giants, asterisks very red ($r - i > 2.0$ giants) and very small diamonds, giant carbon stars. The solid lines are quadratic fits to the points. Only in $g$, where one sees a strong dwarf-giant separation, is there significant spread, amounting to 0.03 or so peak-to-peak in this sample.

Figure 5.
RMS errors in fitting the loss function with a quadratic using the synthetic magnitude differences. The labelling and image center statistics are is the same as for Figure 2. Using colors results in fits worse by a factor of about 3 than the best possible fitting quadratic, but again at airmasses less than 1.5 the errors are better than about two percent. Note that the errors in the calibrating broadband photometry are assumed here to be zero.

Figure 6
Same as Figure 5, but with 2 percent assumed errors in $g - r$ and $r - i$. These curves are essentially exactly reproduced by adding 1.4 times the assumed color errors to the values

in Figure 5 in quadrature. At an airmass of 1.5, the contribution of the color errors already dominates even for very good seeing, and the errors are better than about three percent over most of the range, especially for seeing worse than about 1.4 arcseconds, typical for SDSS spectroscopy.

Figure 7
A set of curves plotting the RMS deviation of the loss function from its mean value in $X$, and hence the RMS spectrophotometric error if no correction for refractive losses is made. The curves are for the seeing values of the previous plots. The seeing values are, from bottom to top at $\sec z = 1.5$: 1.0, 1.2, 1.4, 2.0, and 1.65 arcseconds. The decrease for large seeing is caused simply by the fact that for very large images the centering becomes irrelevant. For seeing in the range 1.4-2 arcseconds and airmasses of 1.2-1.5, conditions under which most of the SDSS data are taken, the errors are 4 to 8 percent.

Figure 8
Same as Figure 6, but with 1 percent assumed errors in the colors. Here the color errors are less important relative to the intrinsic fitting errors, but the resulting RMS spectrophotometric errors are better than 2 percent for representative seeing values for all airmasses less than 1.5, and barely worse than 1.5 percent over most of the typical range of conditions for the SDSS.

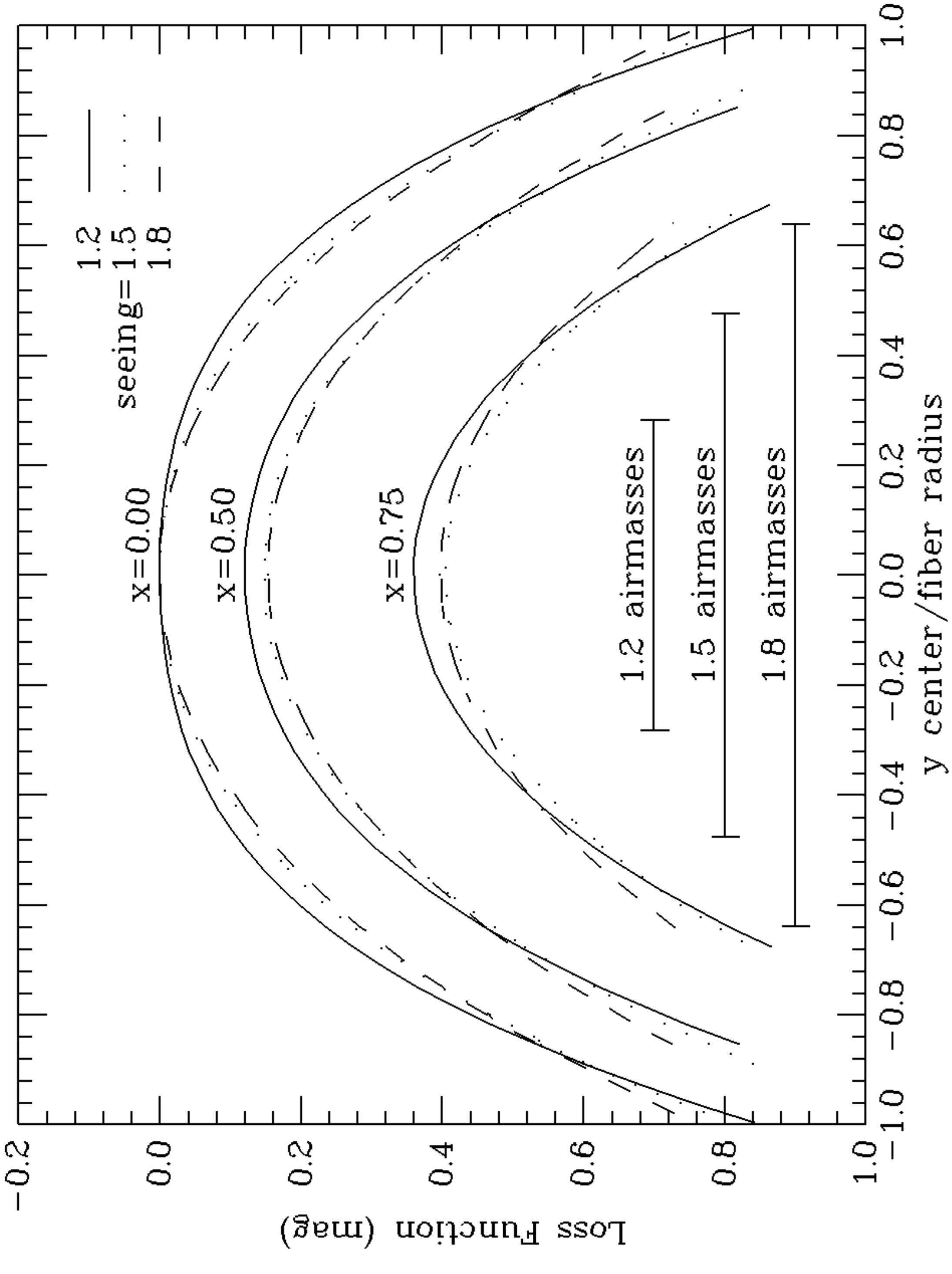
Loss Function (mag)
y center/fiber radius
seeing=1.2
1.5
1.8
x=0.00
x=0.50
x=0.75
1.2 airmasses
1.5 airmasses
1.8 airmasses

Figure 1

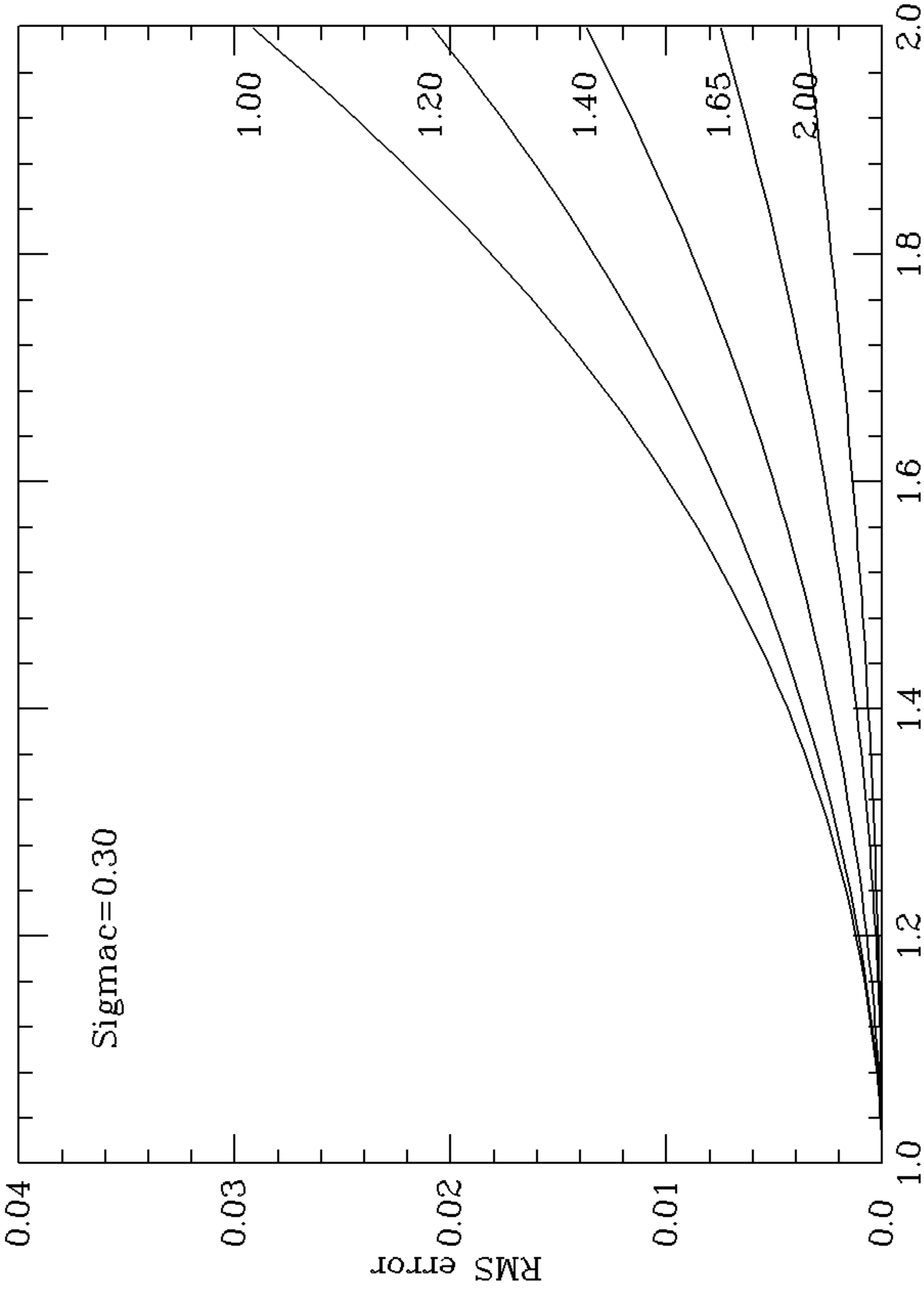

Sigmac=0.30
1.00
1.20
1.40
1.65
2.00
RMS error
0.0
0.01
0.02
0.03
0.04
sec z
1.0
1.2
1.4
1.6
1.8
2.0


Figure 2

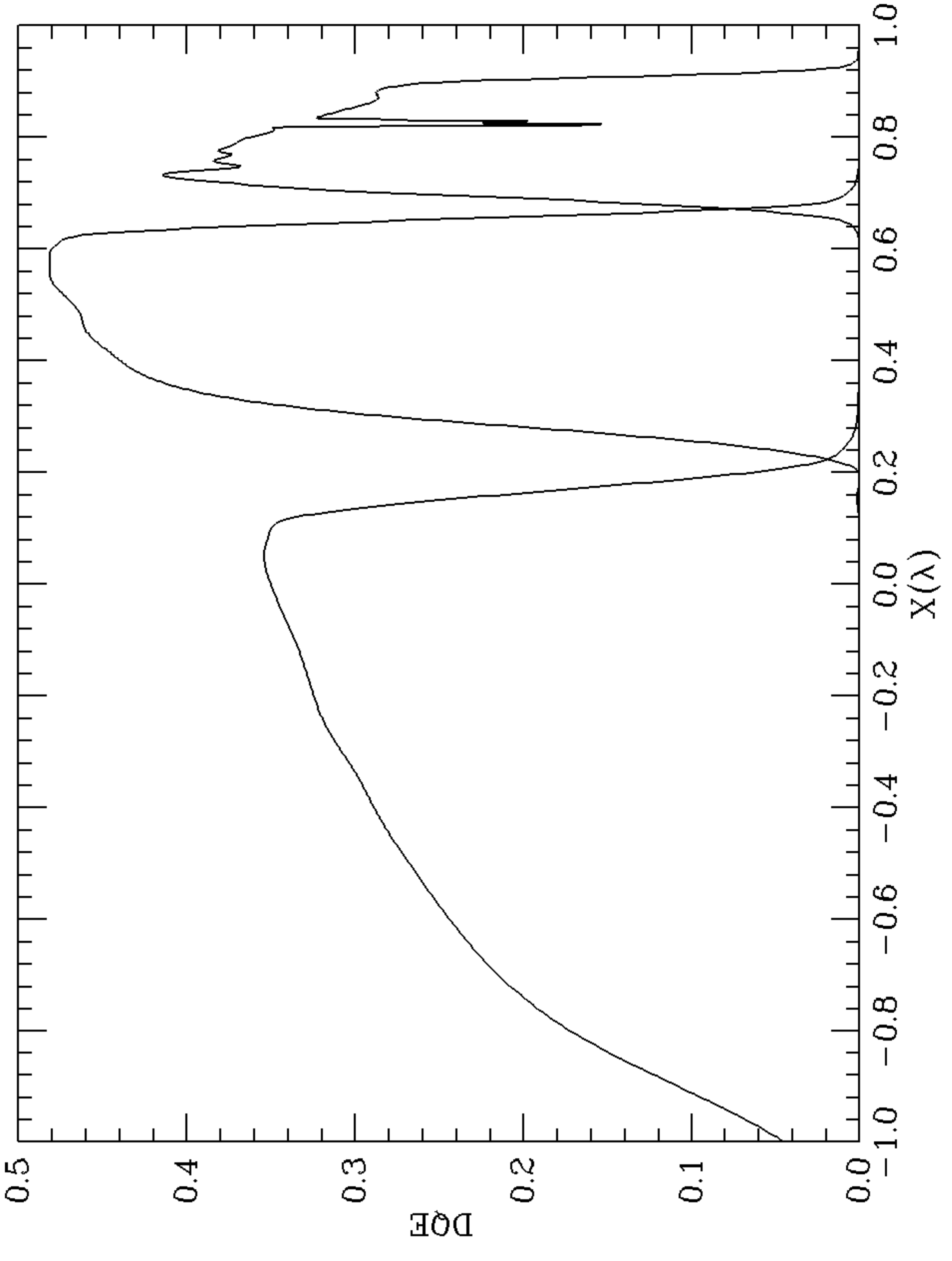


Figure 3

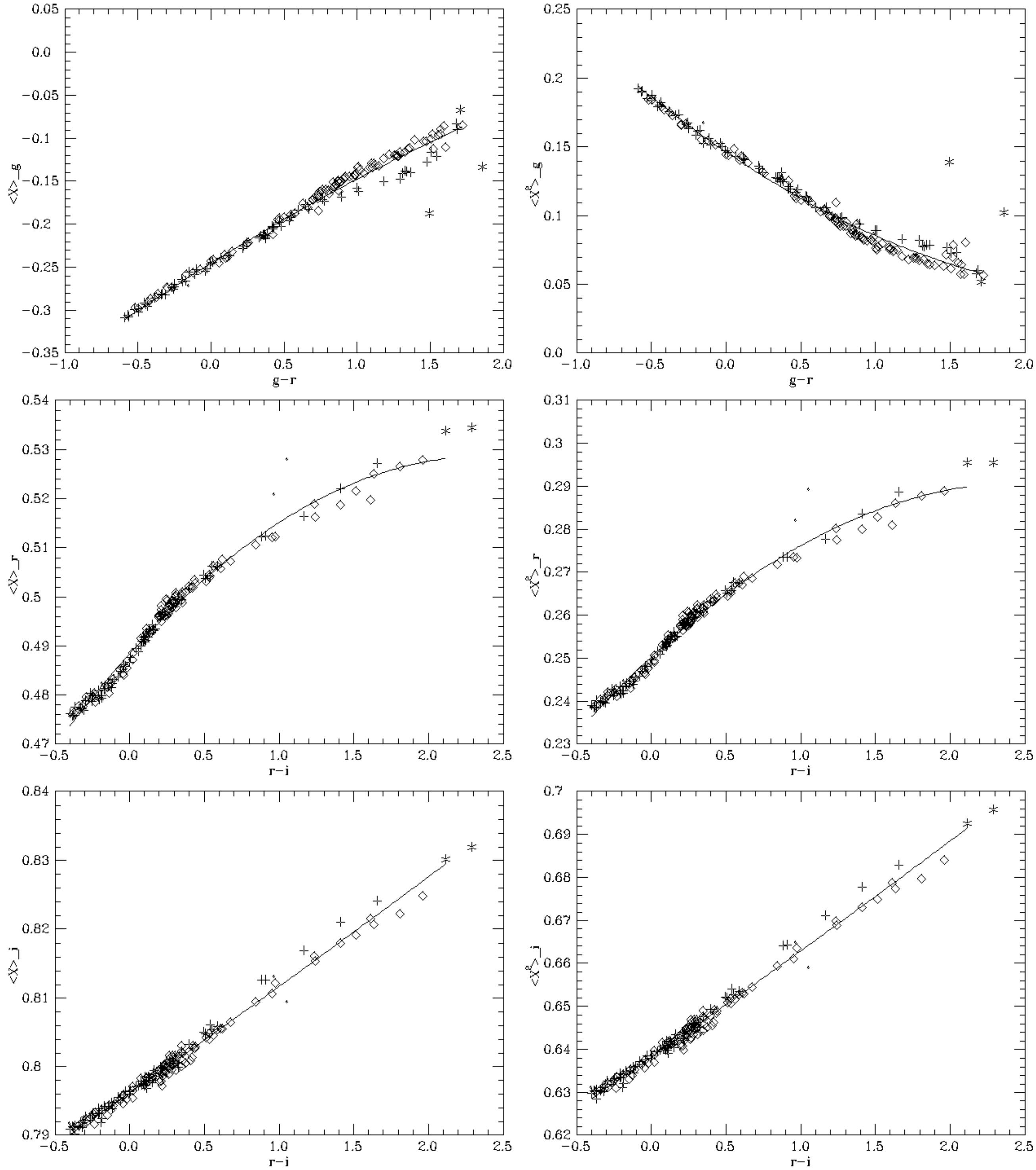


Figure 4

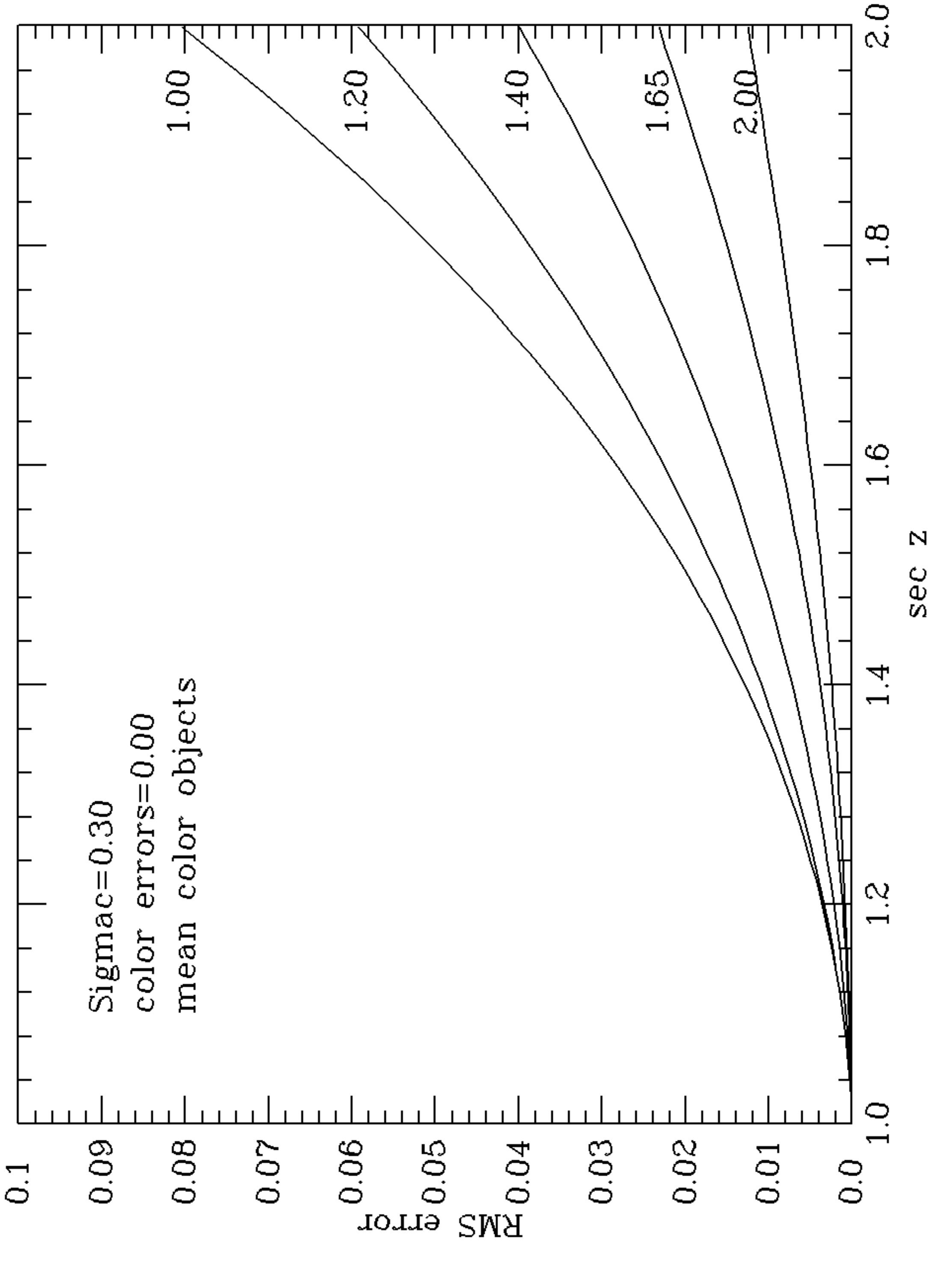
Sigmac=0.30
color errors=0.00
mean color objects
1.00
1.20
1.40
1.65
2.00
sec z
1.0
1.2
1.4
1.6
1.8
2.0
RMS error
0.0
0.01
0.02
0.03
0.04
0.05
0.06
0.07
0.08
0.09
0.1

Figure 5

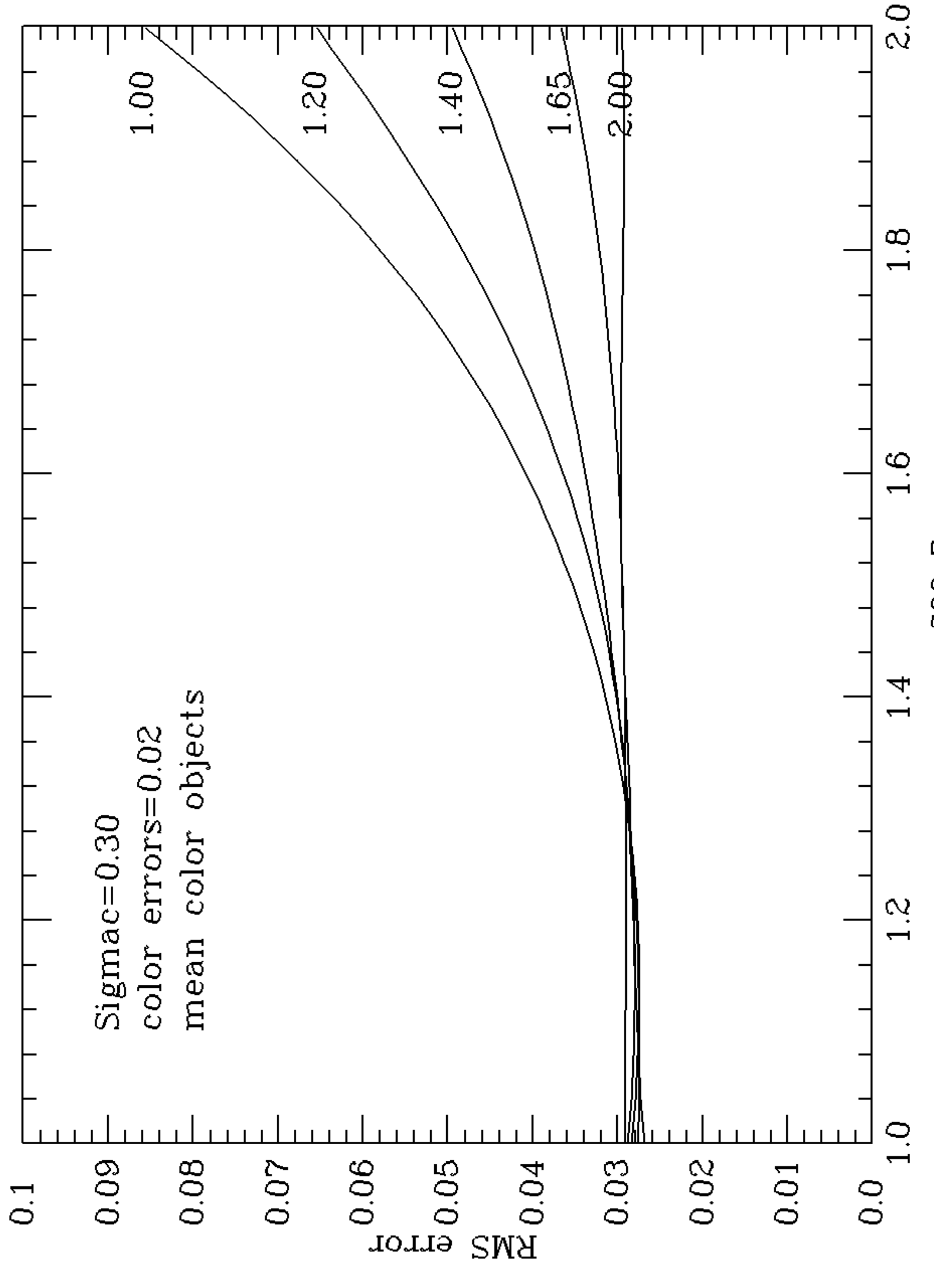

Sigmac=0.30
color errors=0.02
mean color objects
1.00
1.20
1.40
1.65
2.00
sec z
RMS error
1.0
1.2
1.4
1.6
1.8
2.0
0.0
0.01
0.02
0.03
0.04
0.05
0.06
0.07
0.08
0.09
0.1


Figure 6

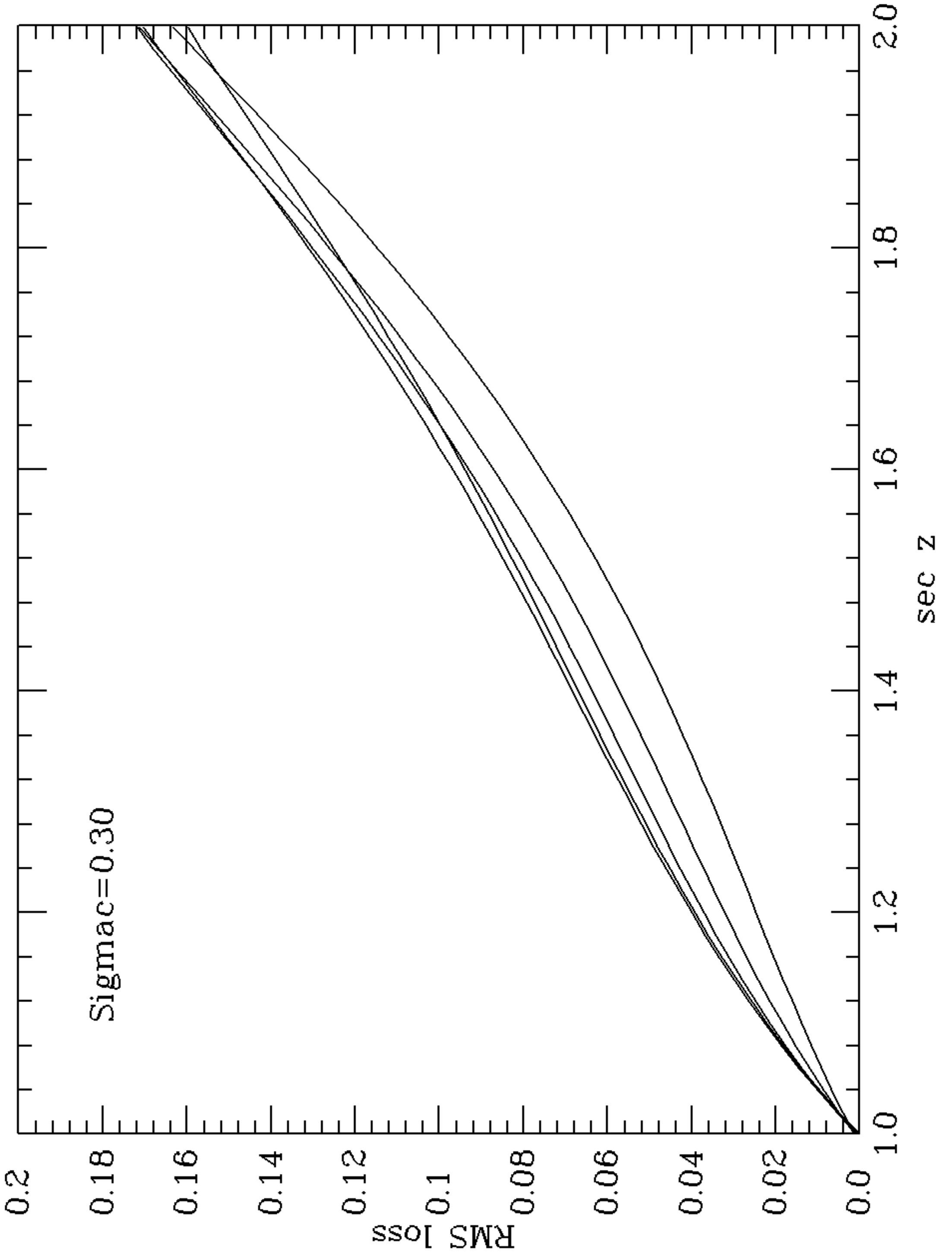

Sigmac=0.30
sec z
RMS loss
1.0
1.2
1.4
1.6
1.8
2.0
0.0
0.02
0.04
0.06
0.08
0.1
0.12
0.14
0.16
0.18
0.2


Figure 7

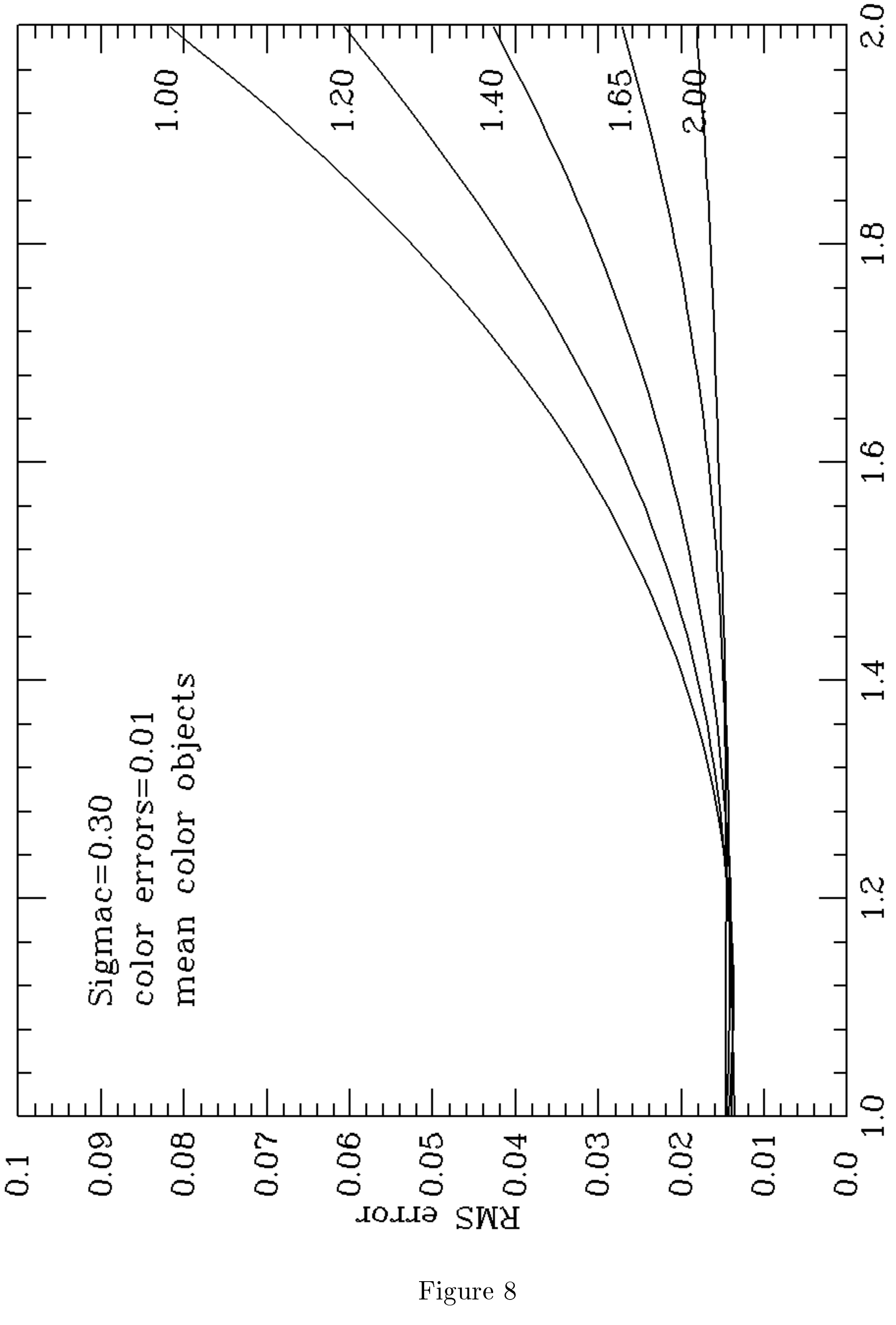
Sigmac=0.30
color errors=0.01
mean color objects
1.00
1.20
1.40
1.65
2.00
sec z
RMS error
1.0
1.2
1.4
1.6
1.8
2.0
0.0
0.01
0.02
0.03
0.04
0.05
0.06
0.07
0.08
0.09
0.1

Figure 8